INVESTIGATION INTO BRINELL HARDNESS TEST APPLIED TO ROCKS

Abdelaziz BOUTRID, Salim BENSEHAMDI

Faculty of Earth Sciences, Mining Department, Annaba University, Algeria

Reçu le 12 Février 2013 – Accepté le 14 Novembre 2013

Résumé

Le travail de recherche réalisé montre l'utilité de l'essai de dureté de Brinell pour l'évaluation de la résistance de la roche. Les essais étés réalisés sur des échantillons obtenus à partir des puits OMN602 et OMN 402 à Hassi Messaoud, pour différentes profondeurs allant de 1900m jusqu'à 2900m. Il est bien connu que l'essai de dureté de brinell dans le domaine de génie mécanique peut êtres utilisé pour les roches d'une manière similaire qu'aux métaux. Des relations empiriques utiles entre la dureté de brinell et la résistance des propriétés physico-mécanique de la roche ont été trouvées.

Mots clés : *Dureté de Brinell, Critère de rupture, Contrainte compression uniaxial, essais triaxiaux, Angle de Friction, Cohésion*.

Abstract

The research work carried out shows the utility of brinell hardness for evaluating the rock strength . Tests were carried out on samples obtained from Hassi Messaoud OMN602 and OMN402 wells , at different depths ,rangings from 1900m to 2900m.

It is well known the brinell hardness in mechanical engineering, can be used on rocks in the same way as that of metals. Useful emperical relations between brinell hardness and the strength properties of the rock were obtained.

Key words: *Brinell Hardness; failure criteria, uniaxial compressive strength, Triaxial Tests; Angle of Friction, Cohesion.*

ملخص

هدا البحث المسطر يختبر نفعية تجربة صلابة برينال لتقييم قوة الصخور المتحصل عليها من آبار حاسي مسعود بئر OMN602 و OMN402 على مختلف الاعماق من 1900م الى 2900م.

من المعروف جيدا أن تجربة برينال تستعمل في الهندسة الميكانيكية . و يمكن استعمالها في الصخور بنفس الطريقة كما تستعمل في المعادن .

تم الحصول على علاقات تجريبية مفيدة بين صلابة برينل و قوة المقاومة و الخصائص الفيزيائية والميكانيكية للصخور.

الكلمات المفتاحية : صلابة برينال، خصوصية القصور، مقاومة الانضغاط أحادي المحور، تجاري ثلاثي المحور، زاوية الاحتكاك، تماسك.

1. Introduction :

The hardness of a mineral is directly related to its chemistry and atomic structure, and reflects to some extent the physical and mechanical properties of the mineral. Hardness is a quality which is readily appreciated but not easily described quantitatively. Various tests have been developed to assess hardness, most of which measure the resistance of the material to scratching or indentation. Mohs proposed a scale of hardness employing a standard set of ten minerals to which relative hardness numbers were allocated [1]. The hardness of a test object is assessed by observing whether or not it is scratched by one of the mineral standards. Scratch hardness may be a useful tool for a quick but rough assesment and has the advantage that no instrumentation is required, however, it leaves much to be desired as a basis for quantitive measurement and is rarely used in engineering. The instrumentation used in determining rock hardness has been developed from indentation techniques for measuring hardness in metals, minerals and other materials that are assumed to be homogeneous. Hardness is expressed in arbritary units depending on the design and application of the measuring instrument. The NCB Cone Indenter [2,3] has been used in the field of rock mechanics to give an indication of rock hardness. Correlations of compressive strength and hardness of Coal Measure rocks has been performed by Szlavin [4] who related uniaxial compressive strength with cone indenter hardness. Investigations into the experimental criteria for classification of rock substances conducted by Coates [5] suggested the possibilty of using some empirical test, such as a hardness or rebound test, to estimate rock strength. Accordingly, Van der Vlis [6] applied the Brinell hardness test, well known in mechanical engineering [7], to rock samples and showed that it could be used as a practical criterion for rock classification. He went on to suggest the existence of an empirical relationship between the Brinell hardness number and the elastic moduli of rock. Ball-point penetrometer tests on rock, previously applied by Huitt and McGlothlin [8] in studies of the deformations occurring during the propping of hydraulic fractures, also point to hardness as a useful indicator to rock properties. As reviewed in the opening chapter, Geertsma [9] proposed that the Brinell hardness test may also be used to assess particle-influx risk. The determination of rock hardness is therefore an important concept in rock mechanics. Brinell hardness, however, is not a fundamental property of a material; it has no qualitative value except in terms of a specified load applied in conjunction with a specific diameter of ball indenter.

This study is primarily to investigate the validity of the Brinell hardness test applied to rock, and establish if a relationships exists between Brinell hardness and the mechanical properties of Hassi Messaoud well OMN602 and OMN402.

2- Test Theory:

The Brinell hardness of a rock may be measured in the same way as that of metals, namely subjecting a sample of the material to a predetermined load via a spherical steel indenter and measuring the diameter or depth of the resulting indentation. The Brinell hardness number (BHN) is defined as the ratio (L/A), where (L) is the applied load in kilogram's and (A) is the spherical surface area of the indentation in square millimeters. This ratio is constant for a given material only when the applied load and indenter diameter are constant.

The Brinell hardness number may then be calculated from the following relationships:.

$$BHN = \frac{L}{(\pi D/2)(D - \sqrt{D^2 - d^2})} \qquad (1)$$

Or

$$BHN = \frac{L}{\pi D h} \qquad (2)$$

Where:

BHN = Brinell hardness number (kg/mm2).
L = Applied Load (kg)
D = Diameter of Ball Indentater *(mm)*
d = Diameter of Indentation *(mm)*
h = Depth of Indentation *(mm)*

3- Development of Brinell Test Apparatus and Procedures:

To apply the Brinell hardness test to rock, lower loads than would be used for testing metal are required while the diameter of the ball indenter is also generally smaller. Accordingly, the use of a standard Brinell tester would not be suitable for testing small samples of rock. As a standard Brinell tester was not available for modification, it was therefore necessary to either design or modify existing departmental equipment for use as a Brinell tester. Two items of equipment appeared suitable for modification: these being an NCB cone indenter which was modified for use as a portable tester, and an oedometer which was adapted for use as a laboratory tester. The necessary modifications to these instruments and the test procedures developed are given below.

3.1-Modified NCB Cone Indenter:

The instrument in its original form measures the penetration of a tungsten carbide tipped cone into a rock fragment under a constant force. The applied load is measured by the deflection of a calibrated steel strip clamped within a steel fraise (Figure.1). The penetration of the cone into the sample is measured and used to give a 'cone indenter

number' which is related to the compressive strength of the rock under test. The modification consisted of replacing the conical indenter by a 5.5 mm diameter hardened steel ball. Due to use of an alternative shape of indenter, it was necessary to recalibrate the instrument. This was accomplished by the application of a series of weights to the steel strip via the ball indenter and noting the respective deflections indicated by the dial gauge reading. A thin metal platten was placed between the indenter and the steel strip to simulate the 'bridging' of a rock sample. The calibration rig is shown in Figure 3. The rotating vernier gauge on the standard instrument was scaled in divisions of 0.025 mm. To provide greater accuracy in reading indentation depths, these divisions were further divided to produce divisions of 0.005 mm.

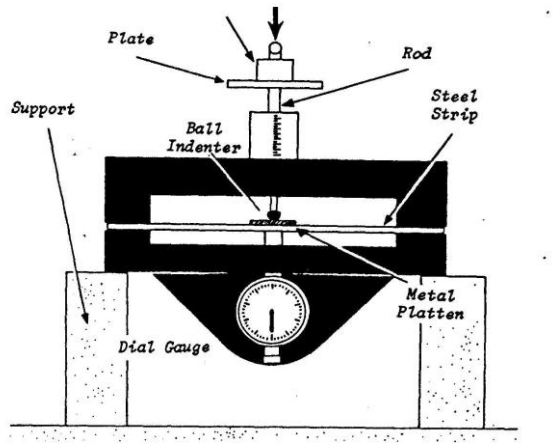

Figure 1: Calibration Rig used for Modified Cone Indenter

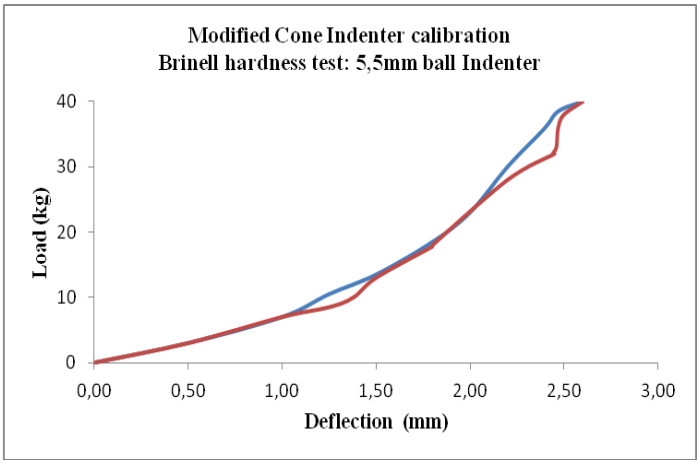

Figure 2: Calibration Graph for Modified Cone Indenter

The unit was calibrated with respect to applied load in stages of 2 kg up to a maximum of 40 kg. The weights applied carefully to reduce the effect of shock loading. The results are presented graphically in Figure 3.4. It can be seen from the graph that the measured deflection of the steel strip was not linear, the higher load producing a lower rate of change of deflection. This was considered to be due to the steel strip offering a greater resistance to bending at elevated loads. Slight hysteresis was also found to be present at higher loads.

3.2- Test Procedure:

Based on experience gained with the instrument, the following test procedure was established. Sample preparation was minimal with the cut-off sections of the core plugs being used for testing. The only preparation required was to smooth the faces of rock disk with emery paper. It was found that confining the rock disk with a plastic cable tie prevented premature tensile failure when used in conjunction with a thin metal platten, the platten being placed between the sample and the steel strip. Accordingly1 this technique was adopted throughout each test. To reduce the effect of surface irregularities, the hardness was determined from the difference in penetration between two load levels. The test procedure was as follows:

(a) The sample and platten were inserted into the device and the ball indenter brought into contact by rotation of the vernier. The dial gauge was zeroed at this point.

(b) The vernier was then slowly and evenly rotated until a reading of 1.28 mm (D1) was indicated on the dial gauge. This corresponded to a load of 10 kg. The vernier reading (M1) was noted.

(c) The vernier was gently rotated further until a reading of 2.20 mm (D2) was indicated on the dial gauge. This corresponded to a load of 30 kg. The vernier reading was again noted (M2).

(d) The depth of the resulting indentation was obtained from the following relationship:

$$\text{Depth} = (M2 - M1) - (D2 - D1) \qquad (3)$$

Two further tests were generally performed on each sample, taking care not to place the indenter on the same spot twice. The average indentation depth was then obtained. The Brinell hardness number was then calculated from equation (2), with L= 20 kg and D= 5.5 mm.

3.3- Modified Oedometer:

An oedometer is an device which is normally used to measure the consolidation of clay or soils over a period of time. The modification to this piece of apparatus consisted of replacing the existing loading arm with an alternative arm incorporating a threaded socket into which a steel ball indenter and holder was fitted. Three holders incorporating respective ball diameters of 1.59 mm, 3.17 mm and 5.5 mm were made. The modified apparatus is illustrated in Figure.3.The standard oedometer dial gauge was replaced by a more accuate gauge reading to 0.002 mm. The loading beam of the oedometer increased the applied load to the sample by a factor of 10:1 (i.e. a weight of 1 kg applied on the pan was equivalent to 10 kg applied to the sample via the loading arm.)

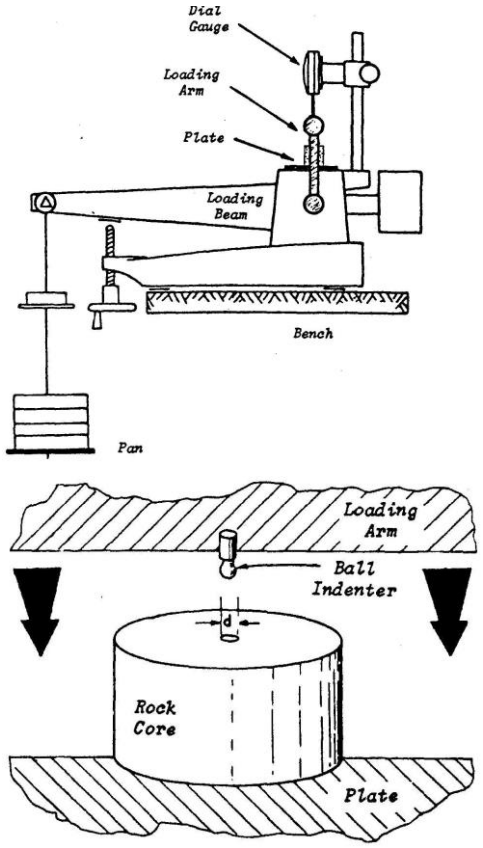

Figure 3: Diagram of Modified oedometer

3.4 -Test Procedure:

The Brinell hardness tests performed using the modified oedometer were conducted on one inch core plugs which had been prepared for mechanical property testing. The prepared sample was confined with a plastic cable-tie to reduce the possibility of failure during the test. The sample was placed on the oedometer load plate and the ball indenter rested on the core surface. Care was required to ensure that the loading arm, core sample and dial gauge were in-line with respect to each other. A retaining load of 1 kg (10 kg app, i.e. corresponding to an applied sample load of 10 kg) was placed on the pan and the dial gauge set to zero. This served to reduce the effect of surface irregularities. A 0.5 kg weiglit (5 kg app) was then added to the pan and the dial gauge reading taken. The load was increased in increments of 0.5 kg (5 kg app) Up to e maximum of 4 kg (40 kg app) and the indentation was read after each incremental increase in load.

In most cases, the penetration of the ball indenter under load into the core samples was not instantaneous. To minimize this source of error, several dial readings were recorded after a load was applied, and when it appeared the reading was constant, that reading was taken as the final depth of indentation. Each sample was subjected to three indentation tests. The place at which the ball indenter rested was chosen at random, however, no tests were conducted at or near the edge of the core sample as this could result in sample failure. After each test the point of penetration was marked and no subsequent test was made in or adjacent to the marked point. A correction-factor test was then conducted to determine the deflection inherent in the apparatus without embedment for various loads. In this test, the ball indenter and holder were removed and substiuted by an empty holder. The holder was then brought into contact with the load plate and the dial gauge set to zero. The deflection of the apparatus was then determined under the same compressive loads as for the Brinell test. This deflection was then subtracted from the total deflection obtained from the Brinell test to obtain the true depth to which the ball-point had penetrated the core sample. No correction was made for strain in the core sample as this was considered to be negligable.

The BHN for each load increment was calculated from equation (2), the average value obtained for each of the indentation tests was again averaged and was designated the Brinell hardness of the rock.

4-Comparison of typical results obtained from each instrument :

A series of tests were performed on Hassi Messaoud well similar rock types to compare the hardness values obtained from the above apparatus. Two types of rock were tested: a red, coarse grained sandstone and a white, fine grained sandstone. Three samples of each rock type were tested on each instrument, three tests being performed on each sample. Both instruments were fitted with a 5.5 mm ball indenter.

4.1- Results using modified cone indenter:

Red Sandstone: The test results for the three red sandstone samples are presented in Table1. The average Brinell hardness number for this rock type was found to be 21.5.
White Sandstone: The Brinell hardness test results for this rock type are given in Table 2. From this table, it can be seen that the average Brinell hardness number using the modified cone indenter was 59.3.

4.2- Results Using Modified Oedometer:

Red Sandstone: The results for the red sandstone are presented in Table 3. The average Brinell hardness number for this rock was measured to be 23.9.

White Sandstone: The results for the white sandstone are given in Table 4 where an average Brinell hardness number of 65 was indicated.

	D2 (mm)	Dl (mm)	M2 *(mm)*	Ml *(mm)*	Depth *(mm)*	BHN
Test #1	2.20	1.28	3.174	2.205	0.049	23.62
Test #2	2.20	1.28	3.410	2.435	0.055	21.05
Test #3	2.20	1.28	3.398	2.420	0.058	19.96
Test #4	2.20	1.28	3.278	2.305	0.053	21.84
Test #5	2.20	1.28	3325	2.355	0.050	23.15
Test #6	2.20	1.28	*3.375*	2.400	0.055	21.05
Test #7	.2O	1.28	3.535	2.565	0.050	23.15
Test #8	2.20	1.28	3.315	2.335	0.060	19.29
Test #9	2.20	1.28	3.311	2.335	0.056	20.67
Red Sandstone Average Brinell hardness Number 21.50						

Table 1: Brinell hardness Results for Red Sandstone Using a Modified NCB Cone Indenter

	D2 (mm)	Dl (mm)	M2 *(mm)*	Ml *(mm)*	Depth *(mm)*	BHN .
Test #1	2.20	1.28	3.395	2.455	0.020	57.87
Test #2	2.20	1.28	3.484	2.545	0.019	60.92
Test #3	2.20	1.28	3.490	2.550	0.020	57.87
Test #4	2.20	1.28	*3.165*	2.225	0.020	57.87
Test #5	2.20	1.28	3.293	2.355	0.018	64.31
Test #6	2.20	1.28	3.439	2.500	0.019	60.92
Test #7	0.2O	1.28	3.093	2.154	0.019	60.92
Test #8	2.20	1.28	3.136	2.195	0.021	55.12
Test #9	2.20	1.28	*3.165*	2.225	0.020	57.87
White Sandstone : average Brinell hardness number = 59.30						

Table 2: Brinell hardness Results for White Sandstone Using a Modified NCB Cone Indenter

	Load (Kg)	Depth of indentation (mm) Test 1	Test 2	Test 3	BHN
Sample #1	5	0.007	0.009	.013	30.70
	10	0.029	0.035	.025	19.41
	15	0.043	0.043	.038	21.09
	20	0.050	0.052	.045	23.69
	25	0.058	0.061.	.056	24.83
	30	0.069	0.072	.075	24.07
Sample #2	5	0.008	0.010	0.011	29.94
	10	0.030	0.029	0.027	20.19
	15	0.041	0.043	0.040	21.00
	20	0.049	0.052	0.048	23.32
	25	0.057	0.062	0.056	24.81
	30	0.070	0.073	0.074	24.00
Sample #3	5	0.009	0.010	0.012	28.00
	10	0.028	0.031	0.023	21h17
	15	0.042	0.044	0.038	21.09
	20	0.052	0.053	0.045	23.15
	25	0.060	0.060	0.057	24.52
	30	0.071	0.072	0.069	24.55
Average Brinell hardness number 23.86					

Table 3: Brinell hardness Results for Red Sandstone Using a Modified Oedometer

	Load (Kg)	Depth of indentation (mm) Test 1	Test 2	Test 3	BHN
Sample #1	5	0.004	0.004	.004	71.64
	10	0.009	0.009	.009	62.69
	15	0.013	0.013	.013	68.39
	20	0.018	0.017	.017	65.41
	25	0.021	0.020	.020	71.64
	30	0.032	0.024	.025	63.57
Sample #2	5	0.005	0.004	.005	62.01
	10	0.010	0.010	.009	59.87
	15	0.014	0.014	.013	63.52
	20	0.019	0.019	.018	62.01
	25	0.023	0.022	.022	64.78
	30	0.027	0.026	.025	66.78
Sample #3	5	0.004	0.004	.004	72.34
	10	0.009	0.008	.010	64.31
	15	0.013	0.014	.014	63.52
	20	0.019	0.018	.019	62.01
	25	0.023	0.023	.024	62.01
	30	0.028	0.027	.028	62.76
Average Brinell hardness number 64.96					

Table 4: Brinell hardness Results for White Sandstone Using a Modified Oedometer

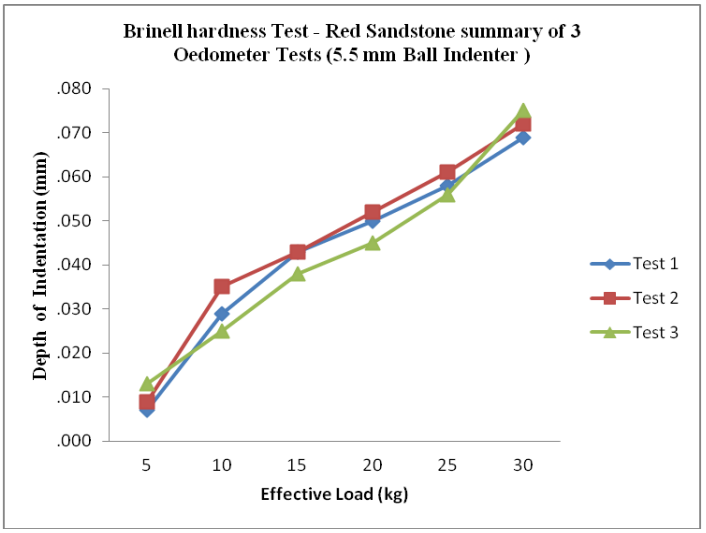

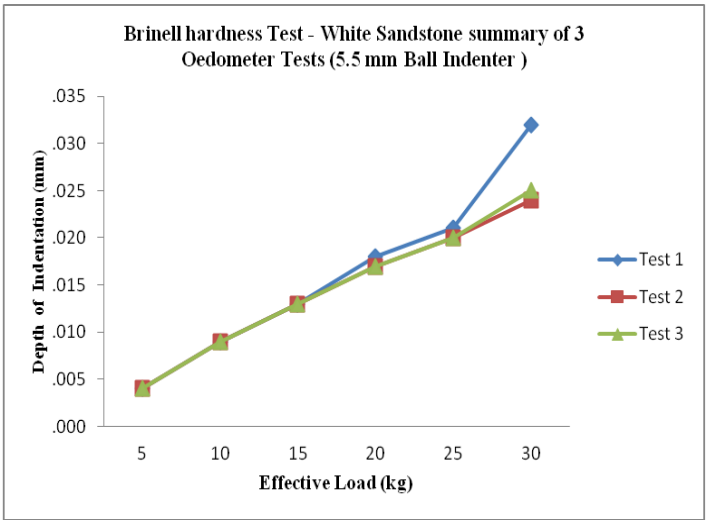

Figure 4: Repeatability of Brinell hardness results using modified oedometer

4.3- Discussion of Results:

From the results presented above, and from numerous unpublished tests, it was apparent that the modified cone indenter provided a lower Brinell hardness number than the modified oedometer, i.e. for the same sample and applied load, the penetration depth measured by the modified cone indenter was greater than the oedometer. The size of sample used in the modified cone indenter could be a contributory factor as a small rock (disk) as used in this test would generally be weaker than a larger sample and therefore be more susceptible to indentation. The main source of error, however, was considered to be in the reading of the vernier gauge. In the standard form, the vernier read to 0.025 mm. The addition of a secondary scale provided an accuracy of 0.005mm, however, reading to a greater accuracy required visual estimation. Accordingly, the modified cone indenter required a degree of operator experience to obtain satisfying results. This effect was more apparent with harder samples where the measurement of penetration depth was more critical. A source of error with the modified oedometer test was in the application of additional weights to the pan. If care was not taken during this operation, the ball indenter could be (shock loaded) which would have the effect of prematurely increasing the depth of indentation and would therefore provide unrealistic results. From the above results, it can be concluded that the modified oedometer provided more repeatable results than the modified cone indenter. In general, however, the repeatability of the test measurements depended on the homogeneity of the sample which was tested. Figure .4 illustrates a set of typical modified oedometer test results for both the white and red sandstone samples. It can be seen that test repeatability was superior with the fine grained white sandstone than with the coarser grained red sandstone.

Although the modified oedometer provides more repeatable results, the modified cone indenter is nevertheless a useful instrument for determining Brinell hardness as it is portable and easy to use, the test samples need little preparation and the results are comparable with the modified oedometer.

5. Determination of mechanical properties :

5.1 Introduction

Sandstone core samples from Hassi Mouassoud wells were available for analysis, these being from sectors OMN/6 and OMN/4 respectively. Accordingly, the following tests were conducted:

(a)Density

(b) P-Wave Velocity

(c) Multi-Failure-State Triaxial tests on strain gauged samples, giving a Mohr's envelope, Static Young's Modulus and Poisson's Ratio at a range of effective confining stress values.

(d) Brinell Hardness

5.2 Sample Preparation:

The mechanical property tests described in this section were performed using one inch diameter plugs which were obtained from the industry standard 4 inch diameter core. During the laboratory coring operations water was used as a lubricant for sandstone sample while an air-flush was used for the shale samples. The ends of the core plugs were trimmed with a diamond saw mounted on a surface grinder before being ground smooth on a lapping machine. A

specimen length to diameter ratio of 2.5:1 was used throughout while the tolerances recommended by Hawkes and Mellor [10] and by the International Society of Rock Mechanics [11].The controls on specimen geometry were intended to ensure that under the action of the testing machine, a predictable, uniform stress was induced in the central section of the specimen, remote from the end effects at the plattens.

5.3 Density:

Rock density was determined from measurements of test specimen volume and weight. The length and diameter of the cylindrical specimens were measured using a digital vernier gauge reading to 0.01 mm, enabling their volume to be determined. The specimens, air dried for 7 days after trimming, were also weighed on a precision balance reading to 0.001 g. Specimen density was then determined by dividing weight by volume.

5.4 P-Wave Velocity:

P-Wave velocity was determined from the time taken for P-wave transmission through the specimen. The equipment shown schematically in Figure 5 was utilized [12], the transmission time being interpreted from the oscilloscope trace shift of the received P-wave caused by introducing the specimen between the transmitting and receiving transducers.

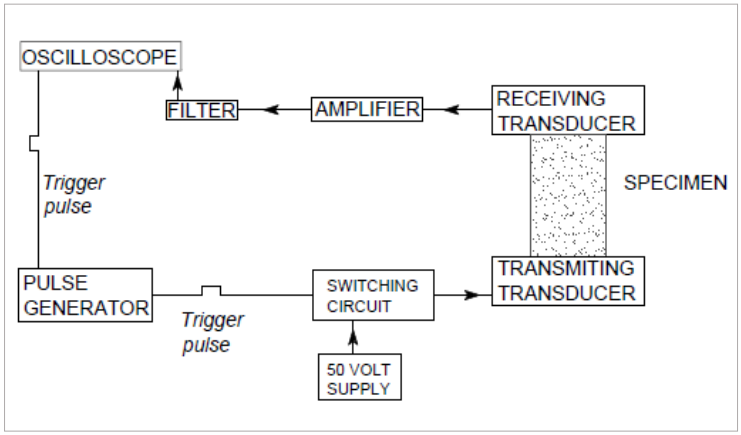

Figure .5. Schematic diagram of equipement used to mesure P-wave velocity

5.5 Multi-Failure-State Triaxial Tests (Specimen Strain Gauged) :

These tests were conducted using a standard Hoek Triaxial Cell rated to 10000 psi (69000 kPa), confining pressure being developed with a hand pump and the axial load being developed by a servo-controlled hydraulic testing machine. Each specimen was strain gauged with diametrically opposed pairs of active vertical and horizontal strain gauges. External dummy gauges on a sandstone core were used to complete the bridges, strain being read on digital meters via strain gauge amplifiers. Connection to the active gauges were made with strips of brass rather than insulated leads as normally used. This system worked well and overcame some of the difficulties experienced with premature lead failure, enabling strains to be monitored in some cases up to 6500 psi (45000 kPa).

5.5.1 Specimen Testing Procedure :

A confining pressure was applied and held constant, while the axial load was increased, the resulting axial strain in the specimen being detected by a linear displacement transducer measuring closure between the loading plattens of the testing machine. The output of the transducer was fed to the X *axis* of an XY recorder, while the axial load applied to the specimen was fed to the Y axis. Strain softening caused flattening of the curve traced. This indicated the onset of failure, and the axial load was noted. The confining pressure was then increased and the axial load increased again until strain softening was detected. Repitition of this procedure up to a confining pressure of 5000 psi (34500 kPa) enabled several failure states to be obtained for each specimen, as shown in Figure 6.

The procedure was usually continued with the confining pressure being reduced in increments to 2500 psi (17250 kPa) , along with a comparable decrease in axial load. The specimen axial load was then increased to cause failure and to produce a residual strength value at a confining pressure of 5000 psi (34500 kPa)

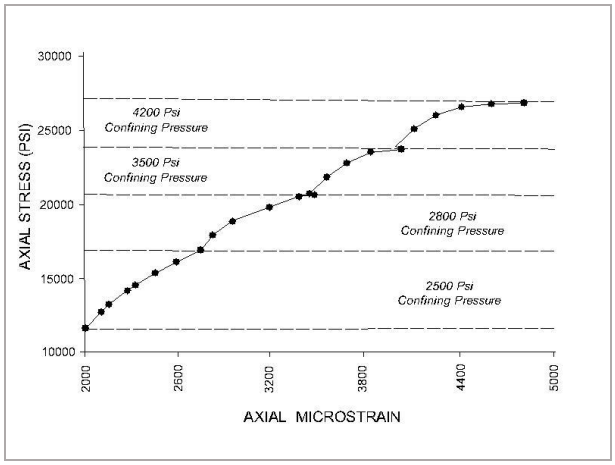

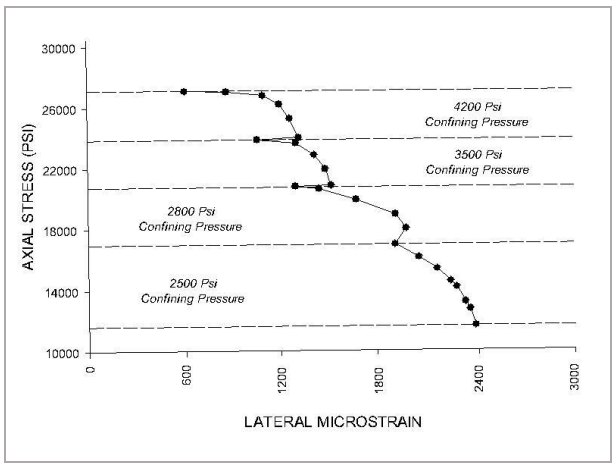

Figure 6: plot of axial & lateral microstrain at various confining pressures (sample 2071.86m)

5.5.2 Internal Angle of Friction and Projected Cohesion :

The multi-failure-state strength data was analysed graphically by the computer program MC-PLOT which was purposely written by the author. The input to the program consisted of the peak strength and confining pressure values for the various failure states which were obtained directly from the XY plot. A failure envelope was then constructed by plotting a series of Mohr's circles. A typical MC-Plot output is presented in Figure.7 the angle of internal friction was measured directly from computer plot with the apparent cohesion was obtained from the intersection of the failure envelope with the shear strength axis.

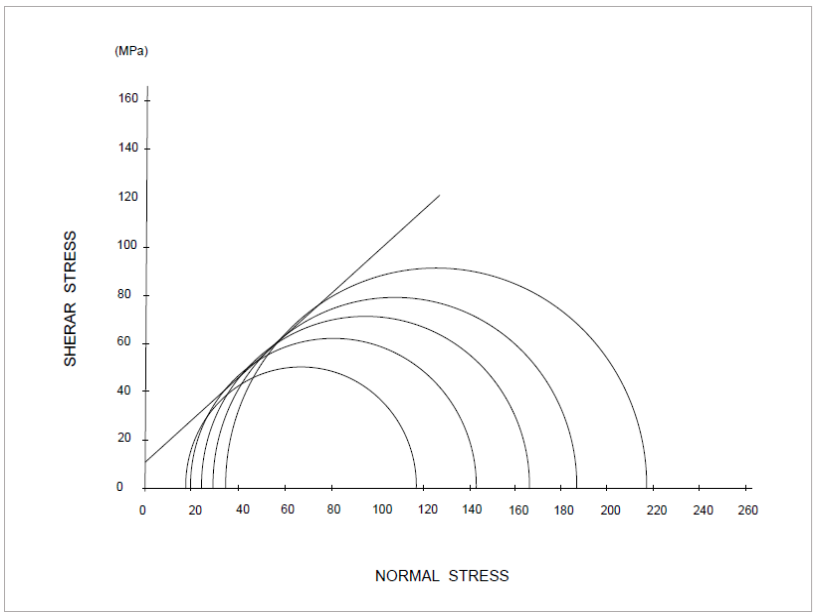

Figure .7 typical MC-PLOT output (Triaxial multi-failure state Mohr circle plot sample 2071.86m)

5.5.3 Triaxial Stress Factor:

The triaxial stress factor is possibly one of most important parameters in assessing the behavior of soft rocks around an excavation [13], it is defined by the following equation:

$$\sigma_1 = \sigma_0 + K\sigma_3 \quad (4)$$

Where

Where

σ_0 = unconfined compressive strength

σ_1 = failure load

σ_3 = Confining pressure

K = Triaxial stress factor

And is related to the angle of internal friction (α) by the expression :

$$K = \frac{1+Sin\ \alpha}{1-Sin\ \alpha} \quad (5)$$

The triaxial stress factor for each sample was calculated from the above equation using the angles of internal friction determined from section 5.5.2

5.5.4 Uniaxial compressive strength:

Due to insufficient core samples available for testing, values of uniaxial compressive strength were derived from the Mohr- Coulomb relationship [14], Viz.

$$C_0 = \frac{2\,S_0\,Cos\,\alpha}{1-Sin\ \alpha} \quad (6)$$

Where

S_0 = the cohesion of the rock

C_0 = uniaxial compressive strength

5.5.5 Young's Modulus and Poissons Ratio:

Specimen strain data obtained in conjunction with the multi-failure triaxial tests was processed using a spreadsheet program, the following theory being used to determine Static Young's Modulus and Poisson's Ratio.

Consider the change in strain from ξ_{Z_1} toξ_{Z_2} that occurs in the Z direction (i.e. along the axis of the test specimen) due to a change in stress from σ_{z_1} to σ_{z_2} the confining stress $\sigma_X = \sigma_Y$ being held constant.

Given that,

$$\xi_{z_1} = \frac{1}{E}(\sigma_{z_1} - 2\upsilon\sigma_x) \quad (7)$$

Where

E = young's modulus

υ = Poisson's Ration

And that similarly

$$\xi_{Z_2} = \frac{1}{E}(\sigma_{z_2} - 2\upsilon\sigma_x) \quad (8)$$

Then the change in strain

$$\xi_{Z_2} - \xi_{Z_1} = \frac{1}{E}(\sigma_{z_2} - 2\upsilon\sigma_x) - \frac{1}{E}(\sigma_{z_1} - 2\upsilon\sigma_x) \quad (9)$$

$$E = \frac{\sigma_{z_2} - \sigma_{z_1}}{\xi_{Z_2} - \xi_{Z_1}} \quad (10)$$

Now consider the change in strain in the X direction due to a change in σ_z, $\sigma_x = constant$

Given that:

$$\xi_{X_1} = \frac{1}{E}(\sigma_X - \upsilon(\sigma_y - \sigma_{z_1})) \quad (11)$$

And that:

$$\xi_{X_2} = \frac{1}{E}(\sigma_X - \upsilon(\sigma_Y - \sigma_{z_2})) \quad (12)$$

Then the change in strain:

$$\xi_{X_2} - \xi_{X_1} = \frac{\upsilon}{\sigma_Y}(\sigma_{z_1} - \sigma_{z_2}) \quad (13)$$

$$\upsilon = \frac{E(\xi_{X_2} - \xi_{X_1})}{\sigma_{z_1} - \sigma_{z_2}} \quad (14)$$

Plotting graphs for ξ_X for increasing σ_z with σ_X= σy constant as shown in Figure 10 enabled the linearity of the stress-strain relationships assumed in the above equations to be confirmed, and equations (10) and (14) to be applied to the determination of Static Young's Modulus and Poisson's Ratio.

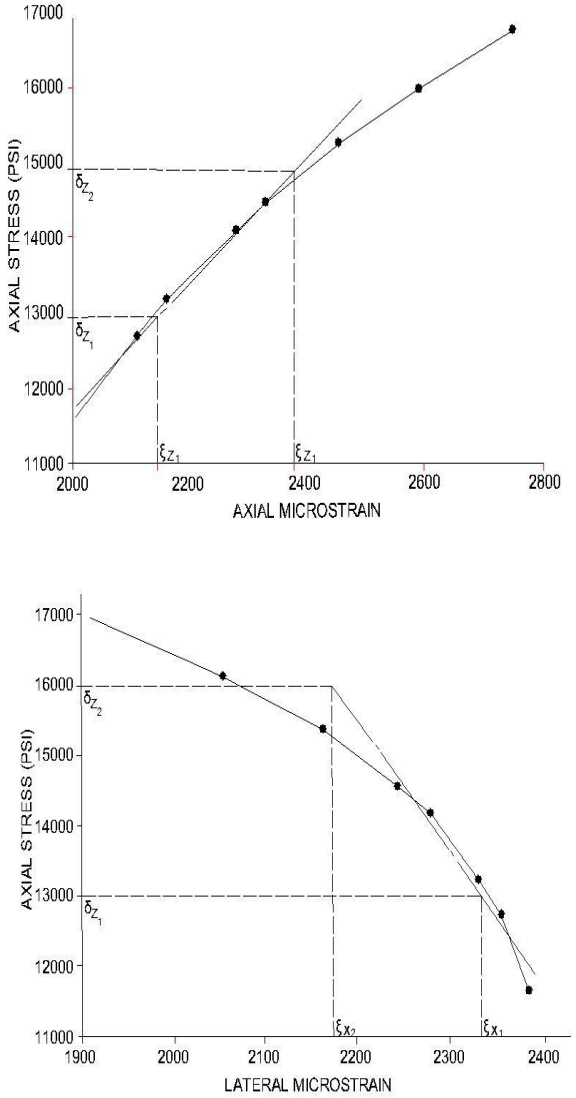

Figure: 8. axial and lateral micro-strain at 2500 psi effective lateral stress (sample 2071m)

5.5.6 Brinell hardness :

As the modified oedometer was not fully commissioned when this testing programme was conducted, a modified NCB cone indenter fitted with a 5.5 mm ball indenter was used to determine Brinell hardness. The experimental procedure outlined in Section 3.2 was followed. The off-cuts of the core plugs were used to provide disks for testing. Due to the short length of the core plugs, however, four of the nine samples from well OMN-602 were not tested, as top priority was given to obtaining the recommended triaxial specimen length.

5.6 Mechanical Property Results:

The results for the above tests are presented in Tables 5 and 6 for wells OMN-602 and OMN-402 respectively.

Sample Depth M	Sample Density g/cm^3	P-Wave Velocity M/s	Young's Modulus Mpa	Poisson's Ratio	Internal Angle of Friction	Triaxial Stress Factor	Apparent Cohesion Mpa	Uni Comp Strength Mpa	Brinell hardness *(kg/mm^2)*
2768.79	2.155	1621.685	23442.17	0.43	27.0	2.66	8.50	27.74	4.1
2772.45	2.139	1455.46	14478.99	0.26	29.5	2.94	8.99	30.85	*4.6*
2776.415	2.045	719.495	21373.75	0.49	195	2.00	1.99	5.66	1,5
2778.855	2.119	1475.285	21373.75	0.29	*25.0*	2.46	9.99	31.38	7.9
2780.685	2.304	1426.18	29647.45	0.47	28.0	2.77	21.01	69.73	-
2781.905	2.418	*2464.4*	37231.68	*0.49*	32.5	3.32	16.49	60.14	8.9
2785.565	2.333	1387.75	33094.83	0.15	30.0	3.00	15.45	53.68	-
2786.785	2.28	1632.665	25510.60	0.29	35.0	3.69	6.99	26.88	-
2788.31	2.266	1535.98	28268.50	0.31	31.0	3.12	10.50	37.12	-

Table 5: Mechanical property test results – well OMN602

Sample Depth M	Sample Density g/cm^3	P-Wave Velocity M/s	Young's Modulus Mpa	Poisson's Ratio	Internal Angle of Friction	Triaxial Stress Factor	Apparent Cohesion Mpa	Uni Comp Strength Mpa	Brinell hardness *(kg/mm^2)*
2066.98	2.46	1743.68	42747.49	0.25	22.0	2.20	17.85	52.95	23
2070.64	2.32	1583.86	51710.67	0.49	43.0	5.29	11.42	52.55	11
2071.86	2.29	1435.33	53089.63	0.37	41.0	4.81	10.71	47.02	24
2072.78	2.28	1341.69	28268.50	0.31	40.0	4.60	11.42	49	7
2080.1	2.27	1358.16	37921.16	0.38	36.0	3.85	14.28	56.07	12
2084.67	2.29	1472.23	62742.29	0.39	38.0	4.20	27.16	111.39	27
2086.81	2.18	1145.88	42747.49	0.33	37.0	4.02	11.42	45.82	17
2087.72	2.33	1158.08	39300.11	0.29	38.0	4.20	15.71	64.43	12
2091.08	2.22	1451.8	42058.01	0.32	34.0	3.54	24.28	91.34	17

Table 6: Mechanical property test results – well OMN402

5.6.1 Discussion of Results: Well OMN-602:

The density of the sandstones tested ranged from 2.045 g/cm^3 to 2.418 g/cm^3, a variation of 15%. This small variation together with the similarity in grain size of the specimens tested and depth of origin (2768.79m-2788.31m) suggested from previous work that properties of all specimens should be similar [15]. Examination of all test results suggests this to be broadly true. P-wave velocity depends on rock type, porosity, degree of consolidation and the fluid in the pore spaces. Density has been taken as an indication of porosity, the other parameters being assumed constant.

A plot of P-wave velocity against density is shown in-Figure 9. There appears to be a logical trend, P-wave velocity increasing with density. Sample density was also plotted against apparent cohesion Figure 10 and general trend was apparent. The relationship between P-wave velocity and Brinell hardness is illustrated in Figure 11 and a logical trend is evident, P-wave velocity increasing with density. This suggested that a relationship should exist between Brinell hardness and apparent cohesion, however, no such correlation was found. There was also little. Correlation between Brinell hardness and sample density. This may be in some part due to the reduced number of Brinell hardness results obtained. A plot of Young's Modulus against Brinell hardness is shown in Figure 12. From an examination of this graph lit was evident that a greater number of Brinell hardness values would be required before a relationship could be conclusive.

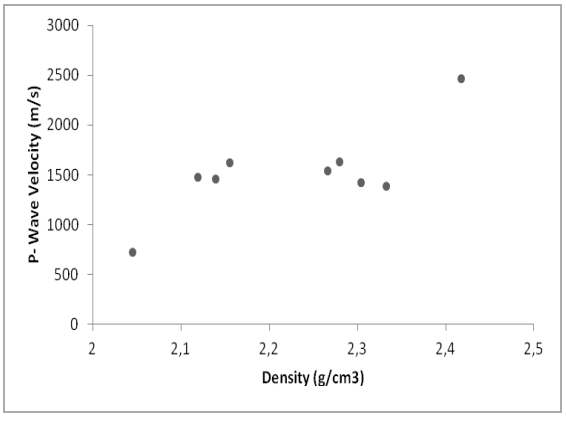

Figure 9 Comparison of P-velocity with sample density

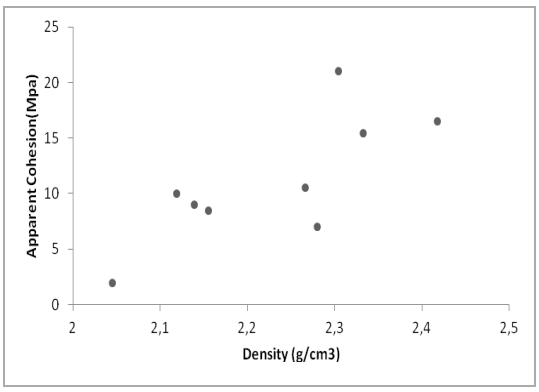

Figure 10 - Comparison of apparent cohesion with sample density

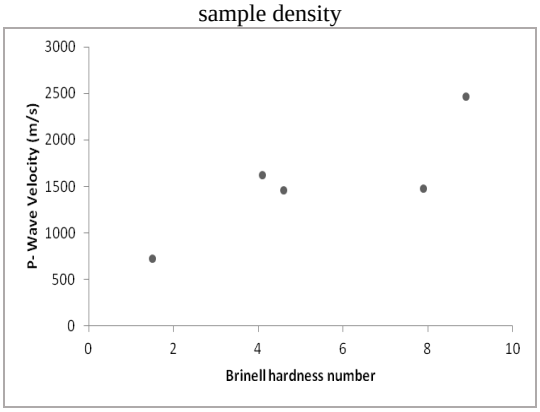

Figure 11 Comparison of P-velocity with Brinell hardness

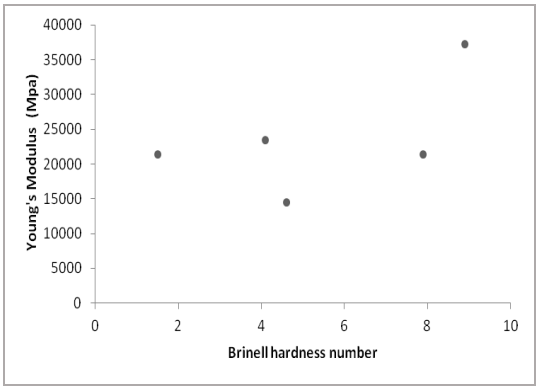

Figure 12 - Comparison of young's modulus with Brinell hardness

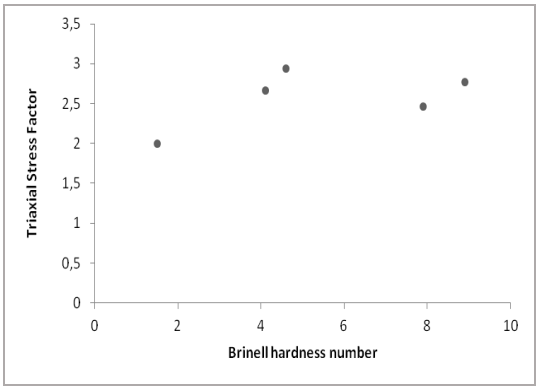

Figure .13.Comparison of Triaxial stress factor with Brinell Hardness

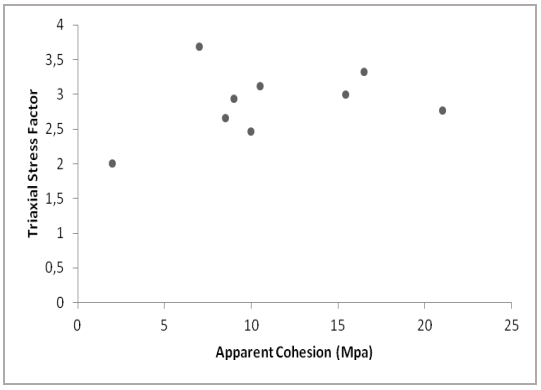

Figure. 14 Comparison of s Triaxial stress factor with apparent cohesion

A plot of Brinell hardness against the triaxial stress factor, as shown in Figure 13, suggested the existence of a relationship. The correlation between the triaxial stress factor and apparent cohesion, however, was less conclusive Figure 14. In general, the values of Young's Modulus and angle of internal friction appeared to be reasonable. There was no apparent correlation between any of these properties with themselves or sample density.

5.6.2 Discussion of Results Well OMN-402:

The density of the rock samples tested ranged from 2.18 g/cm^{3}to 2.46 g/cm^3, a variation of 12%. In general, sample density increased with clay content. The relationship between P-wave velocity and sample density is presented in Figure 15 and a logical trend is apparent. It can be seen from Figure 16, that in this case, no correlation between sample density and apparent cohesion was evident.

There appears to be little relationship between P-wave velocity and Brinell hardness, as evident in Figure 17. A plot of Brinell hardness against Young's Modulus (Figure 18) indicated a definite relationship, the modulus increasing linearly with Brinell hardness. Two samples exhibiting a high clay content were found to deviate from this trend.

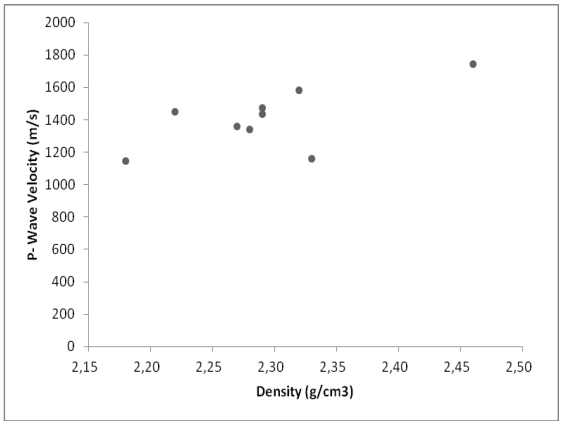

Figure 15: Comparison of P-velocity with sample density

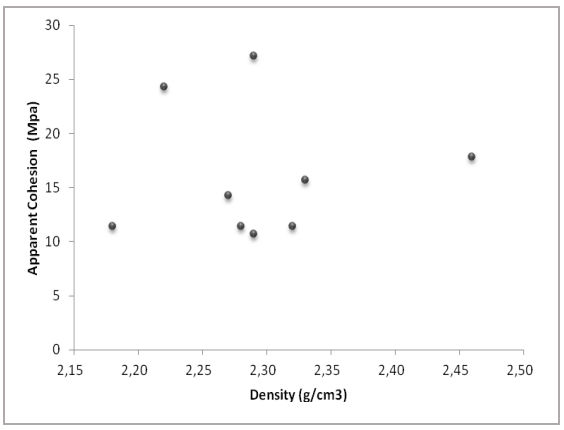

Figure 16: Comparison of apparent cohesion with sample density

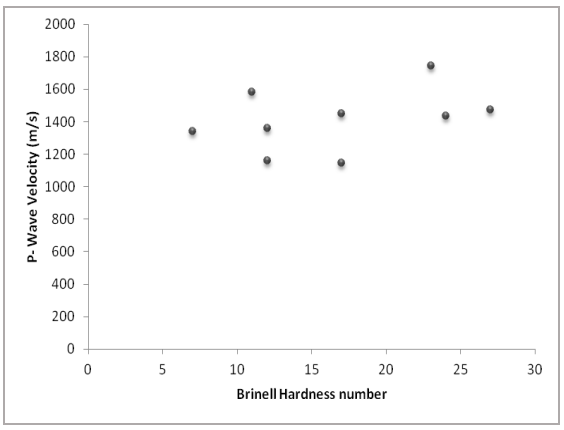

Figure 17: Comparison of P-velocity with Brinell Hardness

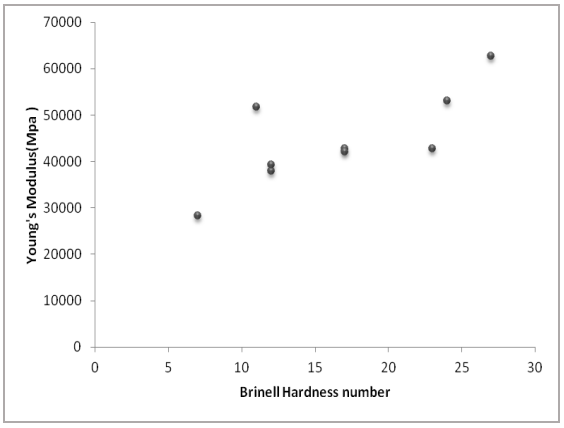

Figure 18: Comparison of young's modulus with Brinell Hardness

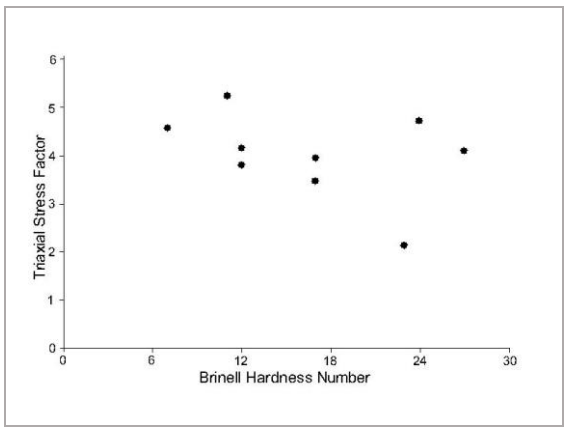

Figure 19: Comparison of Triaxial stress factor with Brinell Hardness

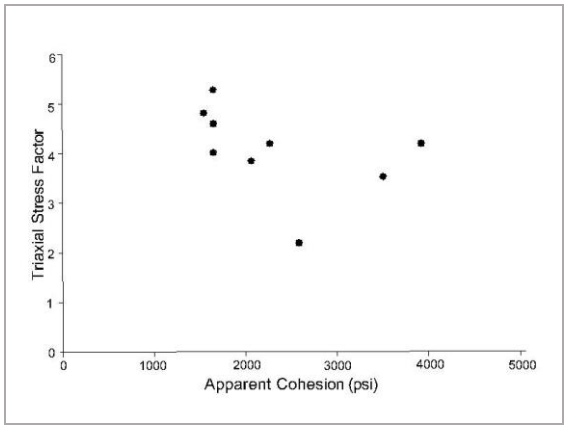

Figure 20:Comparison of s Triaxial stress factor with apparent cohesion

No correlation was found to exist between the triaxial stress factor and Brinell hardness (Figure 19), while the scatter of results obtained from a plot of the triaxial stress factor against apparent cohesion illustrated the absence of a relationship (Figure 20). The values of Young's Modulus and angle of internal friction were of a higher order than the corresponding values from well OMN-602. As with the previous test results, no correlation was found to exist between any of values themselves or with density.

CONCLUSION :

It may be concluded that the Brinell hardness test is a quick and simple method of assessing the properties of a rock. In general, the above results appear to corroborate the existence of a relationship between Brinell hardness and the elastic moduli of rock. A relationship between sample density and P-wave velocity can also be reported, although this is less apparent. As for the other mechanical properties, no direct conclusions can be drawn.

The values of uniaxial Compressive Strength were derived from the Mohr's envelope for each specimen. Ideally, these parameters should have been determined from separate tests. Due to the apparent difficulties in obtaining reservoir core in sufficient quantities to conduct such tests, the results quoted may be considered to give a good indication of the respective properties.

The flattening of the stress-strain curve at different confining pressures (Figure 6) suggests that Young's Modulus and Poisson's Ratio should be determined independently from the Multi-Failure test as it is desirable to obtain stress-strain data from the linear sections of the graph. This, however, would require an additional core sample per test and the availability of such may not always be possible.

The accuracy of the Brinell hardness test may be reduced with samples displaying a high clay content. This possibly due to the variation in sample grain size which, in the case of samples from well OMN 402, had the effect of reducing test repeatability.

The repeatability and linearity of the initial results using the modified oedometer indicate that the instrument is capable of producing accurate hardness values. The attraction with the technique developed is that a prepared core sample can be tested using the apparatus without damage prior to mechanical property testing. This has the advantage of increasing the likelihood of obtaining consistant and meaningful results. The modified NCB cone indenter, although not as accurate as the modified oedometer, is nevertheless of value as a Brinell tester as it is pocket-sized, easy to use and can accept small samples of rock. The instrument is therefore suitable for field use an as the test does not require prepared core samples, it is feasible that it could be used for providing estimates of rock hardness from drill cuttings or other small fragments of rock.

Acknowledgements:

The work described in this paper forms part of the research programme of the Hassi Messaoud SONATRACH. The author is grateful to the Director and his staff for advice and for operating testing machine and to Mr Benameur Mohamed for assistance with specimen preparation and testing.

REFERENCES

[1]. Tabor, D, (1954), Mohrs Hardness scale, A physical interpretation, proceeding physical society of London, sect .B , vol , 67, p 249.

[2,3]. Cone Indenter: new device for measuring rock strength mining and minerals engineering, march 1967, p18 N.C.B cone Indenter M.R.D.E Handbook N°5 (1977).

[4]. Szlarrin, J. relationship between some physical properties of stone determined by laboratory tests, N.C.B, M.R.D.E report Np.19, March (1971).

[5]. Coates, D.F(1964), classification of rocks mechanics, international journal of rock mechanics and mining sciences, Vol, 1, N°3, p 421.
[6]. Van der vlis, A.C, rock classification by simple hardness test, proc. 2nd congress, ISRM(1970)p23-30 1-8.
[7]. Brinell. J. A. 11eme congrès. Internationale. Méthode d'essai, Paris 1900 &
[8]. Huitt, j .L & Mcglothlin B.B, the propping of fractures in formation susceptible to propping sand combedment. Drilland Prod. Practice, 1958, p 115.& relation of formation rock strength to propping agent strength in hydraulic fracturing. Soc. Petrol. Engr. Paper n° 1131 May 1965.
[9].Geertsma,jj (1985) :somme rock mechanical aspects of oil and gaz well completion SPEJ25 P848-856.
[10].Hawkes,I and Mellor, M (1970). uniaxial testing in rock mechanical laboratories engineering geology Vol 4 pp177-285.
[11]. International society for rock mechanics commission on standardization of laboratory and field test (1978).
[12]. ASTM. 1997. Laboratory determination of pulse velocities and ultrasonicelastic constants of rock. ASTM standard D2845-95. In Annual book of standards. American Society for Testing and Materials, West Conshohocken, Pa. Vol. 04.08, pp. 254–259.
[13]. Hobbs, D.W. 1970. the behaviour of broken rock under triaxial compression, Intern. J. Rock Mech. Mining Sci.,vol.7, pp125-148 .
[14]. 14.Hoek, E. and Brown, E.T. 1997. Practical estimates of rock mass strength. Intnl. J. Rock Mech. & Mining Sci. & Geomechanics Abstracts. 34 (8), 1165-1186.
[16]International society for rock mechanics commission on standardization of laboratory and field test (1978).
[17] International Society for Rock Mechanics (ISRM), Commission on Testing Methods (1978), Suggested methods for determining hardness and abrasiveness of rocks.
[18] International Society for Rock Mechanics (ISRM), Commission on Testing Methods(2006), Suggested methods for determining the shore hardness value for rock.
[19] International Society for Rock Mechanics (ISRM), Commission on Testing Methods(1977), Suggested methods for determining water content, porosity, density, absorption and related properties and swelling and slake-durability index properties.
[20]International Society for Rock Mechanics (ISRM), Commission on Testing Methods (1979), Suggested methods for determining the uniaxial compressive strength and deformability of rock materials.
[21]International Society for Rock Mechanics (ISRM), Commission on Testing Methods (1999), Suggested methods for complete stress-strain curve for intact rock in uniaxial compression.
[22] International Society for Rock Mechanics (ISRM), Commission on Testing Methods (1978), Suggested methods for determining the strength of rock materials in triaxial compression.
[23] International Society for Rock Mechanics (ISRM), Commission on Testing Methods (1983), Suggested methods for determining the strength of rock materials in triaxial compression: revised version.